Dynamics of band crossings in the yrast bands of ^{184}Pt and ^{186}Pt

Jing-ye Zhang,[1],[2],[3],[4] F. Dönau,[1],[4],[5] and L. L. Riedinger[4]
[1] *Joint Institute for Heavy Ion Research, Oak Ridge National Laboratory, Oak Ridge, Tennessee 37831*
[2] *Center of Theoretical Physics, Chinese Center of Advanced Science and Technology (World Laboratory), People's Republic of China*
[3] *Institute of Modern Physics, Lanzhou, People's Republic of China*
[4] *Department of Physics, University of Tennessee, Knoxville, Tennessee 37996-1200*
[5] *Zentralinstitut für Kernforschung, Rossendorf, 8051 Dresden, PSF 19, Germany*
(Received 22 September 1989)

Recently much effort has been spent to make the generator coordinator method applicable to problems concerning the dynamics of collective motion at high spin, which goes beyond the possibilities of standard mean field approaches. Using the so-called horizontal expansion, we report in this paper on first calculations about how fluctuations in the triaxial shape can affect the band crossing process among high-spin states in deformed nuclei. For the yrast band in ^{184}Pt, we find that the neutron $i_{13/2}$ pair first starts to align smoothly, but is followed by a sharp alignment of a proton $h_{9/2}$ pair. These two rotational alignment processes take place in a frequency range where there is a strong mixture of shapes with different γ values ranging from -15 to $4°$. The second $\nu i_{13/2}$ pair alignment occurs at a higher frequency ($\hbar\omega \geq 0.45$ MeV). Such theoretical results can explain nicely the double crossing observed in the yrast band of ^{184}Pt and the relevant blocking experiments in the neighboring odd-A nuclei. The result on ^{186}Pt is very different, as only the $\pi h_{9/2}$ crossing is observed in the calculations up to a frequency of 0.40 MeV. This compares well with the data, which indicate one sharp band crossing in ^{186}Pt at low frequency.

I. THE HORIZONTAL EXPANSION

It has been established that the generator coordinator method (GCM) is a powerful approach to the problem of large-amplitude collective motion.[1,2] Particularly in the 1970's, there was much activity in applying the GCM to nuclear collective phenomena. For example, the Faessler group[3] successfully developed the GCM for investigating a variety of collective and collective plus single-particle motions. Our recent effort in treating these phenomena follows a similar spirit. The new element, which we have incorporated into the GCM, is the so-called horizontal expansion (HEX) of the Hamiltonian kernel, as described earlier in detail.[4,5] In this paper we provide a qualitative discussion of the physical basis of HEX in these calculations rather than repeating the original derivation. This paper concentrates on what can be practically achieved by this technique through a calculation of the character of the yrast band crossings in ^{184}Pt and ^{186}Pt.

In the GCM (see Ring and Schuck[6]) the total wave function Ψ is written as a superposition of the generating states $|q\rangle$ that imply the collective variable q as an external parameter. In the calculation presented here, this collective variable is the triaxial deformation γ. The desired weighting function of the superposition that finally determines Ψ is found by solving the Hill-Wheeler equation, which is merely Schrödinger's equation in terms of the chosen generating basis $|q\rangle$. One should be clear on an important and well-known feature of the Hill-Wheeler equation. Since the variable q may, in principle, continuously change, the different generating states do have a finite overlap $\langle q'|q\rangle$. This means that in the GCM one is not working with an orthogonal basis set, unlike the "normal" diagonalization of a Hamiltonian matrix (as in the nuclear shell model).

The horizontal expansion takes advantage of using Hartree-Fock-Bogoliubov (HFB) determinants as generating functions. The collective variables q are to be identified with one or more parameters specifying the involved nuclear mean field, e.g., the deformation parameter(s), the pairing gap, and/or the rotational frequency. Using such parameters as collective variables, q is obviously a good choice, since the nuclear many-body system responds directly to any change of these parameters. For example, the nucleonic orbitals have to be accommodated in an average potential that may be altered in its geometrical shape, in its superfluid properties, or in the angular frequency if it is rotated in space.

Each HFB state $|q\rangle$ can be considered as a quasiparticle (qp) vacuum state with regard to the creation and annihilation operators $a_i^\dagger(q)$ and $a_i(q)$ defined locally at a given parameter point q, where the index i refers to the qp orbital. Any alteration of the mean field parameter q translates into a change of the vacuum state and simultaneously modifies the qp operators belonging to it. Generally, we can define two alternative changes of a given HFB state $|q\rangle$.

(1) "Vertical" changes are obtained by any 2 qp excitation at a given point q, i.e., $|q\rangle \rightarrow [a_1^\dagger(q)a_2^\dagger(q)]|q\rangle$. The vertical changes are characterized by having zero overlap

with the initial state $|q\rangle$. In addition, any 2 qp excitation is normally connected with a nonzero energy jump, since one is abruptly changing the vacuum configuration.

(2) "Horizontal" changes of the HFB state are achieved by shifting the parameter value q, i.e., $|q\rangle \rightarrow |q'\rangle$. The horizontal changes are determined by nonzero overlap with the initial state, thus enabling one to perform quasicontinuous alterations of the initial configuration. (To simplify the calculation, we do not consider here changes simultaneously in both the horizontal and the vertical directions.)

The aim of the GCM is obviously to follow horizontal changes of HFB configurations, i.e., to move *in the direction* of the collective mode under consideration.

The Hamiltonian H can, of course, be expressed in terms of the above local qp operators. Assuming the normal ordering one realizes immediately the following identity when operating on the corresponding vacuum state $|q\rangle$:

$$H|q\rangle = \langle q|H|q\rangle\,|q\rangle + H^{2\ \mathrm{qp}}\,[a_1^\dagger(q)a_2^\dagger(q)]\,|q\rangle + H^{4\ \mathrm{qp}}\,[a_1^\dagger(q)a_2^\dagger(q)a_3^\dagger(q)a_4^\dagger(q)]\,|q\rangle, \qquad (1)$$

where the notation $H^{2\ \mathrm{qp}}$ and $H^{4\ \mathrm{qp}}$ shows the inherent number of quasiparticles in the subsequent bracket. (Because of possible constraints such as angular momentum conservation, the term $H^{2\ \mathrm{qp}}$ might be nonzero.[3]) Equation (1) states only the simple fact that in the expanded Hamiltonian there survive only those terms that have no qp annihilator on the right side. Except for the contributions involving zero, two, and four quasiparticles, all other combinations of the above qp operators vanish in acting on the local vacuum. The 0 qp term is the local expectation value $\langle q|H|q\rangle$, which is often referred to as the static energy or the potential energy surface with respect to variations of the variable q.

Concerning Eq. (1) one should realize that the operation of the Hamiltonian yields a horizontal (0 qp) term as the leading-order part, plus two vertical terms (2 qp and 4 qp). Consequently, we call the decomposition in Eq. (1) the horizontal expansion (HEX).

Now we are in the position to formulate the HEX approximation for the Hamiltonian kernel $\langle q'|H|q\rangle$ that enters the Hill-Wheeler equation. This kernel is the counterpart of the Hamiltonian matrix when referring to an orthogonal basis.

In the crudest approximation (which will be used throughout this paper), one neglects totally the vertical 2 qp and 4 qp terms. Forming the overlap with another HFB state $|q'\rangle$ (which is in the above sense horizontally connected with the initial HFB state), one gets the approximated Hamiltonian kernel

$$\langle q'|H|q\rangle = 1/2\,(\langle q'|H|q'\rangle + \langle q|H|q\rangle)\,\langle q'|q\rangle\ , \qquad (2)$$

which has been symmeterized with respect to the points q and q'.

The building blocks of the Hamiltonian kernel (Eq. 2) are given by the diagonal energy surface $E(q) = \langle q|H|q\rangle$ and the nondiagonal overlap matrix $\langle q'|q\rangle$.

As usual the Hill-Wheeler equation is practically solved by discretizing the collective variable q. This procedure then takes the form of a diagonalization of a nondiagonal Hamiltonian kernel matrix and overlap matrix, and yields automatically quantized energies and solutions. We recall the fact that without any other approximation it is impossible to split the Hamiltonian kernel into kinetic energy and static potential parts. This separation only makes sense when applying the Gaussian overlap approximation (GOA) for the Hamiltonian kernel.[6] According to our experience with realistic HFB states, one can hardly describe the structure of the resulting overlap matrix by a Gaussian shape, especially in regions of level crossings. For collective modes where the overlap matrix behaves smoothly, GOA is applicable, and then the Hill-Wheeler equation assumes the form of a differential equation with kinetic terms and mass parameters. Our approach is to diagonalize the Hamiltonian kernel (2) in a straightforward manner and not apply GOA, which clearly does not invalidate our approach. However, one can still interpret the diagonal elements $\langle q|H|q\rangle$ as potential energy terms (as in the GOA) and relate the nondiagonal elements in Eq. (2) to kinetic effects. Even more relevant for applications is the following option.

The simple structure of the HEX kernel (Eq. 2) allows one to use the techniques and results from the advanced Strutinsky mean field calculations.[7] These calculations not only provide potential-energy surfaces but also yield HFB states parametrized in terms of the desired shape parameters. This option leads to the great advantage of performing GCM calculations without explicit use of complicated effective interactions and without need for a self-consistent HFB procedure. Because of the demonstrated success of the Strutinsky mean field approach in high-spin physics, it seems to be the appropriate basis for the next step of GCM calculations in which the qp states belonging to various shapes and configurations become mixed.

The expression (2) obtained by HEX shows explicitly the important role of the overlap matrix for the coupling of the generator states. The detailed study of the overlap matrix provides a way of surveying the collective motion beyond the usual static information contained in the potential landscape. This is because a sizable overlap between two points q and q' tells us immediately that a direct transition $q \rightarrow q'$ is favored, whereas a small overlap forbids such a direct transition (i.e., in zeroth order). Thus, in rigorous calculations of overlap "trees," there are clearly revealed structural details that otherwise would be smoothed out in a Gaussian overlap approximation. This is particularly true for cases of simultaneous consideration of several degrees of freedom, e.g., in nuclei where the interplay of pairing gap vibrations and various shape fluctuations (axial versus non-axial or reflection asymmetric shapes) are of interest.

In the following, the horizontal expansion (2) is applied in zeroth order to solve the Hill-Wheeler equation

and get the evolution of the eigenstates as a function of rotational frequency. We apply this new approach to investigate the structure of the yrast bands in ^{184}Pt and ^{186}Pt, which have been difficult to understand using conventional techniques.

II. THE OVERLAP MATRIX FOR THE YRAST BAND OF ^{184}Pt

The band crossing process in the yrast sequence of ^{184}Pt has been a puzzle for several years.[8–13] The first measurement[8] on the yrast band of ^{184}Pt led to the conclusion that the large increase in the aligned angular momentum is a result of a neutron $i_{13/2}$ crossing. Kahler *et al.*[9] compared the characteristics of band crossings in ^{185}Au to that in ^{184}Pt and concluded that the rotational alignment of a proton $h_{9/2}$ pair is the dominant effect. More recently, experimental information on the band crossings in the yrast and nonyrast sequences of ^{184}Pt has been compared to that on band crossings in a number of neighboring odd-A nuclei.[10–15] From this more detailed blocking analysis, it can be concluded[10,11] that both of these alignment processes ($\nu i_{13/2}$ and $\pi h_{9/2}$) occur in the range of $\hbar\omega$ from 0.2 to 0.4 MeV, and are responsible for the measured upbend in ^{184}Pt. These experimental comparisons also give some indication (although not conclusive) that the $\pi h_{9/2}$ crossing occurs first, at a slightly lower frequency than $\nu i_{13/2}$. In contrast, many theoretical calculations with Nilsson and Woods-Saxon cranked-shell potentials [including large-scale total Routhian surface (TRS) calculations] indicate that the $\nu i_{13/2}$ pair alignment must occur at a lower frequency than the other. There is another possibility, as pointed out by Bengtsson[14] and discussed also by Carpenter *et al.*,[15] that two neutron $i_{13/2}$ pairs align sequentially (the AB and CD crossings in the standard notation) in this frequency region, without a $\pi h_{9/2}$ pair alignment.

In order to investigate the dynamic aspects of the band-crossing process, we have calculated the overlap matrix for the yrast band of ^{184}Pt. First, the rotational frequency was taken as the collective variable of interest, in order to investigate individually the characteristics of the two types of band crossings for specified deformations. Secondly, we solved the Hill-Wheeler equation numerically by taking deformation and frequency as the generator variables, so that we can trace the evolution of the complete band-crossing process. These overlap functions from both of these calculations may then describe the dynamics of the collective motion.

The total Routhian surface calculation is known to provide the static description of the possible shapes a nucleus may take at high rotational frequency. Such shapes correspond to the TRS minima for any selected frequency. The TRS has been a powerful tool for interpreting high-spin data and predicting specific phenomena, e.g., the expected mass regions for superdeformation. However, such static TRS calculations cannot tell us what the transmission probability between distinct minima in such potential landscapes is. For this purpose, one needs to calculate the distribution function over this TRS to get insight into what path through the deformation-frequency plane the nuclear system is really going to take during an excitation or deexcitation. This means actually accounting for the dynamics of collective processes.

In the specific examples considered here we demonstrate that the overlap matrix is one of the proper instruments to answer the questions raised above. Minima from the TRS calculation for ^{184}Pt are as follows:[11–13,15] the yrast state just before the first band crossing, $\hbar\omega = 0.15$ MeV: $\beta_2 = 0.217$, $\beta_4 = -0.029$, $\gamma = 0$; the neutron $i_{13/2}$ aligned state at $\hbar\omega = 0.15$ MeV: $\beta_2 = 0.218$, $\beta_4 = -0.038$, $\gamma = -15°$; and the proton $h_{9/2}$ aligned state at $\hbar\omega = 0.2$ MeV: $\beta_2 = 0.235$, $\beta_4 = -0.031$, $\gamma = 4°$.

Using the cranking model with the Woods-Saxon potential (including Strutinsky shell corrections), we have obtained the overlaps of the wave functions (i.e., $\langle q|q'\rangle$) between different frequencies over a range of $\hbar\omega = 0.15$–0.45 MeV. These calculations were performed at these three deformation points, without particle-number projection. We find that the dimension of the subspace is two for both the neutron and proton parts of the wave function. This means that there is only one neutron and one proton crossing in this frequency range. The values of these overlaps are plotted in Fig. 1 as a function of frequency. It is clear in Fig. 1 that there is a smooth decrease in the values of the overlaps for the neutron part. This indicates a very gradual change of the neutron configuration over a wide frequency region, starting from $\hbar\omega = 0.2$ MeV for $\gamma = -15°$. This pattern of decreasing overlap is shifted towards higher frequency as γ increases. However, the corresponding $\pi h_{9/2}$ crossing behaves quite

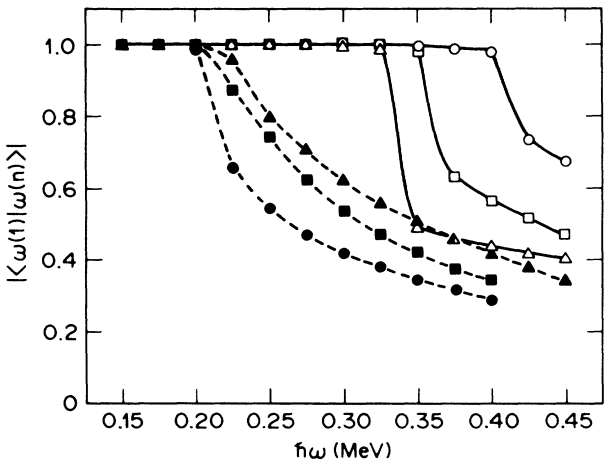

FIG. 1. Calculated wave function overlaps between states with different frequencies for neutron (dashed lines) and proton (solid lines) components in the yrast band of ^{184}Pt, as a function of rotational frequency. Separate calculations were carried out for $\beta_2 = 0.217$, $\beta_4 = -0.029$, $\gamma = 0$ (squares); $\beta_2 = 0.218$, $\beta_4 = -0.038$, $\gamma = -15°$ (circles); and $\beta_2 = 0.235$, $\beta_4 = -0.031$, $\gamma = 4°$ (triangles), as described in the text.

differently. It is much sharper and higher in frequency, starting to occur at $\hbar\omega = 0.325$ MeV for the deformation $\beta_2 = 0.235$, $\beta_4 = -0.031$, $\gamma = 4°$, and at $\hbar\omega = 0.4$ MeV for the deformation $\beta_2 = 0.218$, $\beta_4 = -0.038$, $\gamma = -15°$. In the latter case, i.e., if the neutron $i_{13/2}$ pair is already aligned completely, the difference between the $\pi h_{9/2}$ and $\nu i_{13/2}$ crossings is about 0.2 MeV. Generally speaking, such a difference increases if γ becomes more negative. In contrast, the systematic blocking experiments [10–12,15] in this mass region seem to indicate that these two band crossings ($\nu i_{13/2}$ and $\pi h_{9/2}$) are much closer together in frequency, and that the proton $h_{9/2}$ crossing may occur at a slightly lower value than the neutron $i_{13/2}$ crossing.

In order to investigate fully the competition between these two band-crossing processes, the Hill-Wheeler equation was solved numerically for the nucleus ^{184}Pt by descretizing the collective variables and calculating the overlap matrix. Such a calculation was done with a Nilsson-cranked-shell model with modified parameters[16] κ and μ in two-dimensional (deformation and frequency) space. For simplicity, the coupling between different N shells is neglected, as is usually done.

In the calculation, we included five frequency mesh points (from 0.20 to 0.45 MeV) and eight deformation mesh points, keeping $\epsilon_2 = 0.212$ (the average of the three β_2 values mentioned in the previous paragraph) with γ varying from $-25°$ to $+15°$. A decreasing pairing gap was assumed, i.e., 100%, 80%, and 60% of the odd-even mass difference for $\hbar\omega = 0.20$ and 0.25 (100%), 0.30 and 0.35 (80%), and 0.40 and 0.45 MeV (60%). The results showed that if we take the same cut on the norm eigenvalue, the dimension of the subspace is three to five, varying with frequency. That is, at low frequency there are apparently three distinct configurations that contribute to the wave function of the yrast band. At a higher frequency, there are five contributing configurations, indicating a structure of increased complexity. The general observation for the whole frequency region is that the lowest eigenstates are formed from neither a specific configuration nor of a definite shape but are instead spread over all the deformation mesh points. However, one finds a structural change in the wave function as a function of frequency. This can be seen in Fig. 2, which plots the normalized square of the expanding coefficients of the eigenfunction (amplitude) on the basic HFB determinants with certain values of γ. As shown in Fig. 2, the wave function of the lowest eigenstate is spread over different γ values with the concentration around $-15°$ to $+4°$ at $\hbar\omega = 0.2$ MeV. This concentration shifts to more negative γ with increasing frequency up to 0.3 and 0.35 MeV, where the γ average value equals $-14°$. This means that the neutron $i_{13/2}$ aligned state makes a substantial contribution in this frequency region, whereas afterwards (at higher frequency) the concentration goes to positive γ values, the proton $h_{9/2}$ alignment process clearly becoming dominant. Both alignment processes are thus found to occur at or below a frequency of 0.4 MeV.

As mentioned above, an alternative explanation for the

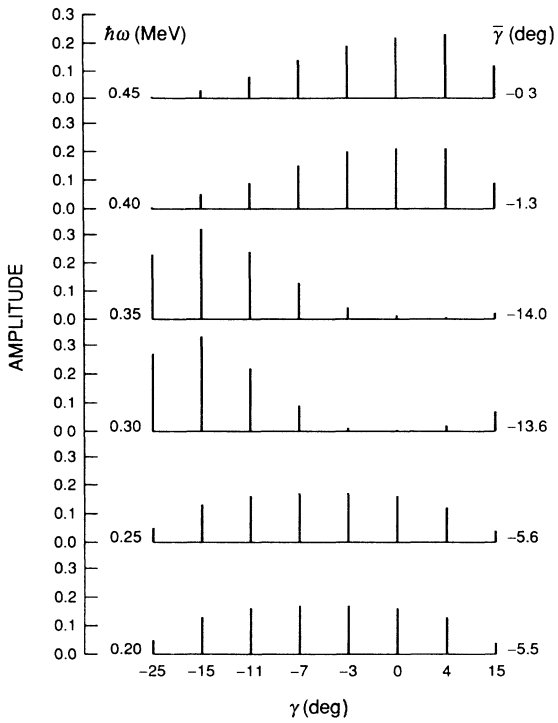

FIG. 2. The structural evolution of the eigenstate as a function of frequency in the yrast band of ^{184}Pt. The basis states have the same ϵ_2 but different γ values, as mentioned in the text. The amplitudes are normalized squared expansion coefficients of the eigenstates, and the γ values are given in degrees.

double band crossing in ^{184}Pt is that there are two $\nu i_{13/2}$ pair alignments.[14,15] In order to carefully check for a second $\nu i_{13/2}$ pair alignment in this frequency region, we performed another calculation where once again the frequency is taken to be the only generator variable, but this time with a different value of the pairing correlation. The γ value is chosen to be $-14°$, which results from the alignment of a neutron $i_{13/2}$ pair. The neutron pairing gap is taken to be small (150 keV), and the proton pairing gap is assumed to be 80% of that for the ground state. We find that the dimension of the subspace for the neutron part is still only two in this frequency region. This means that there is only one band crossing, only one neutron $i_{13/2}$ pair aligned in this frequency region. Consequently, from the calculation in one- and two-dimensional space, one can conclude that the upbend in the yrast band of ^{184}Pt is really caused by the gradual alignment of a neutron $i_{13/2}$ pair followed closely by the sharp alignment of a proton $h_{9/2}$ pair. In ^{180}Pt, however, our calculation shows a second neutron $i_{13/2}$ pair aligned in this frequency region, as described by Bengtsson recently.[14]

It is important to emphasize here that one should be careful in drawing conclusions about the band-crossing mechanism of a transitional even-even nucleus based on the blocking experiments of neighboring odd-A nuclei (e.g., see Ref. 17). This is simply because the even-even

core of the neighboring odd-A nucleus may have a quite different deformation and pairing correlation from that of the even-even nucleus. A quantitative discussion of the difference in deformation among different configurations in odd-A and even-A nuclei was presented recently for this mass region.[15] It shows that the polarization of the extra proton or neutron in an odd-A nucleus does lead to the variation in the crossing frequency of the $\nu i_{13/2}$ and/or the $\pi h_{9/2}$ band compared to the values found in even-even nuclei. Therefore, for a transitional nucleus like ^{184}Pt, the blocking experiments of odd-A neighbors can only tell the existence of certain kinds of band crossings in the neighboring even-even nucleus, but not the exact crossing frequency.

Generally speaking, our calculations show that such a band-crossing phenomenon in ^{184}Pt is a more complicated process than one expected earlier, and explains why the normal cranked-shell model calculations with a constant deformation cannot describe this process properly.

III. THE OVERLAP MATRIX FOR THE YRAST BAND OF ^{186}Pt

The experimental information on the yrast band of ^{186}Pt indicates a band crossing pattern quite different from that in ^{184}Pt. Whereas the yrast band of ^{184}Pt exhibits two strongly interacting band crossings below $\hbar\omega = 0.4$ MeV, that of ^{186}Pt displays a single sharp backbend at $\hbar\omega = 0.24$ MeV.[18] The addition of two neutrons has a profound effect on the nature of the low-frequency band crossings. Blocking comparisons of the alignment features of the $N = 108$ isotones show sharp crossings in the $\pi d_{5/2}$ band of ^{185}Ir (Ref. 19) and in the $\pi i_{13/2}$ band of ^{187}Au (Ref. 20) at frequencies very similar to that of the yrast band of ^{186}Pt. In contrast, the crossings in the $\pi h_{9/2}$ band of ^{185}Ir (Ref. 19) and of ^{187}Au (Ref. 20) are delayed. This leads to the conclusion[19,20] that the $\pi h_{9/2}$ crossing occurs at a low frequency ($\hbar\omega = 0.24$ MeV) for $N = 108$, and that the $\nu i_{13/2}$ crossing seems strongly delayed. However, cranked-shell model calculations cannot produce such a low-frequency $\pi h_{9/2}$ crossing without an unreasonable reduction of the proton pair gap.[15]

We have performed GCM calculations on ^{186}Pt to address this dilemma. In the solution of the Hill-Wheeler equation, mesh points were taken for γ varying from $-40°$ to $+16°$ in steps of $4°$, with a constant $\epsilon_2 = 0.174$. Constant proton and neutron pairing gaps (obtained from a self-consistent calculation for the ground state) were used over the frequency region of interest for the ease of calculation. The results are shown in a plot of the amplitudes as a function of γ and $\hbar\omega$ in Fig. 3. It is clear that the concentration of the wave function shifts to positive γ values already at $\hbar\omega = 0.20$ MeV, which must be indicative of a very low-frequency $\pi h_{9/2}$ crossing. This is in striking contrast to the pattern of the amplitudes shown in Fig. 2 for ^{184}Pt, where the wave function initially shifts to negative γ values (i.e., a $\nu i_{13/2}$ crossing) and then finally moves to positive values ($\pi h_{9/2}$ crossing)

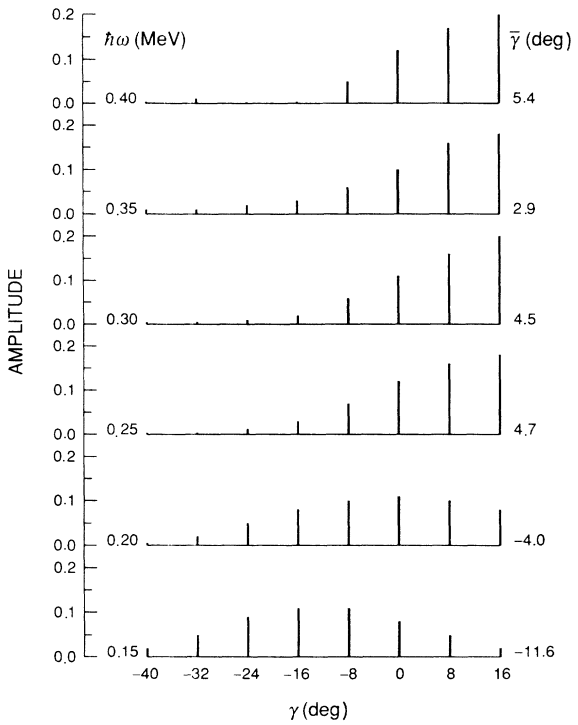

FIG. 3. The structural evolution of the eigenstate as a function of frequency in the yrast band of ^{186}Pt. The basis states have the same ϵ_2 but different γ values, as mentioned in the text. The amplitudes are normalized squared expansion coefficients of the eigenstates, and the γ values are given in degrees.

only at $\hbar\omega = 0.40$ MeV. Indeed, in the calculation shown in Fig. 3, there is no indication of the $\nu i_{13/2}$ crossing up to $\hbar\omega = 0.40$ MeV. The addition of the two neutrons to ^{184}Pt obviously has the effect of greatly increasing the crossing frequency for the $\nu i_{13/2}$ pair, because of an $N = 108$ gap in the single-particle neutron scheme.[15]

The calculations thus seem to verify the experimental proposal[19,20] that the single low-frequency band crossing in ^{186}Pt results from the alignment of a $\pi h_{9/2}$ pair. Such a conclusion would not have been made from the usual type of "static" calculations based on the TRS results. The dynamic aspects of the structure are apparently quite important for these transitional nuclei.

IV. SUMMARY

From a general discussion on the solution of the Hill-Wheeler equation in previous sections, it was seen that significant information is involved in the overlap matrix. From this, one can not only solve the Hill-Wheeler equation numerically by discretization of the continuous generator variables but can also learn much about the dynamical aspects of the collective motion, such as the process of band crossing, the evolution of the eigenstate, and the dimension of the collective subspace. Such a dimension is closely related to the band-crossing mechanism in high-spin physics because it provides information about

the contributing configurations. The calculated overlap matrix in one- and two-dimensional space for the yrast band in ^{184}Pt offers for the first time a more detailed picture describing the band-crossing process. The calculations indicate a smooth neutron $i_{13/2}$ pair alignment closely followed by a sharp proton $h_{9/2}$ alignment, which causes the upbend in the yrast band of ^{184}Pt. In contrast, the yrast band in ^{186}Pt is marked only by the low-frequency $\pi h_{9/2}$ crossing, as the $\nu i_{13/2}$ alignment process moves to much higher frequency.

It is true that the calculations leading to the amplitudes in Figs. 2 and 3 assume $\epsilon_4 = 0$. This simplifying assumption was made to permit the solution of the Hill-Wheeler equation with both deformation (ϵ_2 and γ) and rotational frequency as generator variables. Especially the $\pi h_{9/2}$ crossing is dependent on ϵ_4, which means that one cannot quantitatively stress the position of this crossing relative to that of $i_{13/2}$ neutrons in either Fig. 2 or Fig. 3. However, our main conclusion stands—there is a marked change in the pattern of the wave function from ^{184}Pt (Fig. 2) to ^{186}Pt (Fig. 3), a change that matches the experimental pattern of two low-frequency crossings in ^{184}Pt and only one in ^{186}Pt. The calculations indicate that the change results from a lowering of the $\pi h_{9/2}$ crossing in ^{186}Pt compared to ^{184}Pt.

With this powerful calculational technique, we expect to have the proper theoretical scheme for the investigation of the dynamical aspects of other high-spin phenomena, such as the connection between superdeformed and normal bands, the decay process of the high-K isomers, shape coexistence and pairing isomer[21] phenomena, etc. Large-scale calculations of the overlap matrix and solving the Hill-Wheeler equation in multidimensional space (including deformation, frequency or spin, and pairing degrees) are needed in order to bring new light to the dynamics of high-spin physics.

ACKNOWLEDGMENTS

We would like to thank Dr. R. Bengtsson, Dr. T. Bengtsson, Dr. J. D. Garrett, Dr. I. Ragnarsson, and Dr. P. Semmes for inspiring discussions. The Joint Institute for Heavy Ion Research has as member institutions The University of Tennessee, Vanderbilt University, and Oak Ridge National Laboratory and is supported by them and by the Department of Energy under Contract No. DE-AS05-76ERO-4936 with the University of Tennessee.

[1] D. L. Hill and J. A. Wheeler, Phys. Rev. **89**, 1102 (1953).
[2] J. J. Griffin and J. A. Wheeler, Phys. Rev. **108**, 311 (1957); J. J. Griffin, *ibid.* **108**, 329 (1957); J. J. Griffin and K. K. Kan, Symposium on Physics and Chemistry of Fission, Rochester, 1973 (unpublished).
[3] A. Faessler, F. Grummer, A. Plastino, and F. Krmpotic, Nucl. Phys. **A217**, 420 (1973); K. Goeke, K. Allart, H. Muther, and A. Faessler, Z. Phys. **271**, 377 (1974); S. Krewald, R. Rosenfelder, J. E. Galonska, and A. Faessler, Nucl. Phys. **A269**, 112 (1976); H. Muther, K. Goeke, K. Allart, and A. Faessler, Phys. Rev. C **15**, 1467 (1977); H. -T. Chen, H. Muther, and A. Faessler, Nucl. Phys. **A297**, 445 (1978).
[4] F. Dönau, J. -Y. Zhang, and L. L. Riedinger, Nucl. Phys. **A496**, 333 (1989).
[5] J. -Y. Zhang, F. Dönau, and L. L. Riedinger, in *Proceedings of the Workshop on Microscopic Models in Nuclear Structure Physics, Joint Institute for Heavy Ion Research*, Oak Ridge, 1988, edited by M. W. Guidry *et al.* (World Scientific, Singapore, 1989), p. 237.
[6] P. Ring and P. Schuck, *The Nuclear Many-Body Problem*, (Springer, Berlin, 1980), Chap. 10, and references therein.
[7] R. Bengtsson, S. E. Larsson, G. E. Leander, P. Möller, S. G. Nilsson, S. Åberg, and Z. Szymanski, Phys. Lett. **57B**, 301 (1975); K. Neergard, V. V. Pashkevich, and S. Frauendorf, Nucl. Phys. **A262**, 61 (1976); C. G. Andersson, S. E. Larsson, G. A. Leander, P. Möller, S. G. Nilsson, I. Ragnarsson, S. Åberg, R. Bengtsson, J. Dudek, B. Nerlo-Pomorska, K. Pomorski, and Z. Szymanski, *ibid.* **A268**, 205 (1976).
[8] S. Beshai, K. Fransson, S. Hjorth, A. Johnson, T. Lindblad, and J. Sztarkier, Z. Phys. A **277**, 351 (1976).
[9] A. C. Kahler, L. L. Riedinger, N. R. Johnson, R. L. Robinson, E. F. Zganjar, A. Visvanathan, D. R. Zolnowski, M. B. Hughes, and T. T. Sugihara, Phys. Lett. **72B**, 443 (1978).
[10] A. J. Larabee, M. P. Carpenter, L. L. Riedinger, L. H. Courtney, J. C. Waddington, V. P. Janzen, W. Nazarewicz, J. -Y. Zhang , R. Bengtsson, and G. Leander, Phys. Lett. **169B**, 21 (1986).
[11] L. L. Riedinger, V. P. Janzen, and M. P. Carpenter, Proceedings of the XXII Winter School on Physics, Zakopone, Poland, 1987, edited by R. Broda and Z. Stachura (Institute of Nuclear Physics, Jagiellonianian University, Krakow, Report No. IFJ 1370/PL), Pt. 1, p. 315.
[12] M. P. Carpenter, doctoral thesis, University of Tennessee, 1987.
[13] R. Bengtsson, T. Bengtsson, J. Dudek, G. Leander, W. Nazarewicz, and J. -Y. Zhang, Phys. Lett. **183B**, 1 (1987); (unpublished).
[14] R. Bengtsson, in *Proceedings of the Conference on Contemporary Topics in Nuclear Structure Physics*, Cocoyoc, Mexico, 1988, edited by R. F. Casten *et al.* (World Scientific, Singapore, 1989), p. 317.
[15] M. P. Carpenter, C. R. Bingham, L. H. Courtney, V. P. Janzen, A. J. Larabee, Z. -M. Liu, L. L. Riedinger, W. Schmitz, R. Bengtsson, T. Bengtsson, W. Nazarewicz, J. -Y. Zhang, J. K. Johansson, D. G. Popescu, J. C. Waddington, C. Baktash, M. L. Halbert, N. R. Johnson, I. Y. Lee, Y. S. Schutz, J. Nyberg, A. Johnson, J. Dubuc, G. Kajrys, S. Monaro, S. Pilotte, K. Honkanen, D. G. Sarantites, and D. R. Haenni, Nucl. Phys. **A513**, 125 (1990).
[16] J. -Y. Zhang, L. L. Riedinger, and A. J. Larabee, J. Phys. G **13**, L75 (1987).
[17] J. -Y. Zhang, Proceedings of the International Conference on Nuclear Physics, Berkeley, 1980 (Lawrence Berke-

ley Laboratory Report LBL-11118), p. 317; Nucl. Phys. (China) **3**, 1 (1981).
[18]G. Hebbinghaus, W. Gast, A. Krämer-Flecken, R. M. Lieder, J. Skalski, and W. Urban, Z. Phys. A **328**, 387 (1987).
[19]D. L. Balabanski, W. Gast, G. Hebbinghaus, A. Krämer-Flecken, R. M. Lieder, T. Morek, T. Rzaca-Urban, H. Schnare, and W. Urban, Z. Phys. A **332**, 111 (1989).
[20]J. K. Johannson, D. Popescu, D. D. Rajnauth, J. C. Waddington, M. P. Carpenter, L. H. Courtney, V. P. Janzen, A. J. Larabee, Z. M. Liu, and L. L. Riedinger, Phys. Rev. C **40**, 132 (1989).
[21]I. Ragnarsson, in *Future Directions in Studies of Nuclei Far From Stability*, edited by J. H. Hamilton *et al.* (North Holland, Amsterdam, 1980), p. 367.